Neuron, Vol. 39, 779–791, August 28, 2003, Copyright ©2003 by Cell Press

Drosophila Pod-1 Crosslinks Both Actin and Microtubules and Controls the Targeting of Axons

Michael E. Rothenberg,[1,2] Stephen L. Rogers,[3] Ronald D. Vale,[3] Lily Yeh Jan,[1,2] and Yuh-Nung Jan[1,2,*]

[1] Department of Physiology
[2] Department of Biochemistry
[3] Department of Cellular and Molecular Pharmacology
Howard Hughes Medical Institute
University of California, San Francisco
533 Parnassus Avenue
San Francisco, California 94143

Summary

Actin and microtubules (MTs) are tightly coordinated during neuronal growth cone navigation and are dynamically regulated in response to guidance cues; however, little is known about the underlying molecular mechanisms. Here, we characterize *Drosophila pod-1* (*dpod1*) and show that purified Dpod1 can crosslink both actin and MTs. In cultured S2 cells, Dpod1 colocalizes with lamellar actin and MTs, and overexpression remodels the cytoskeleton to promote dynamic neurite-like actin-dependent projections. Consistent with these observations, Dpod1 localizes to the tips of growing axons, regions where actin and MTs interact, and is especially abundant at navigational choice points. In either the absence or overabundance of Dpod1, growth cone targeting but not outgrowth is disrupted. Taken together, these results reveal novel activities for *pod-1* and show that proper levels of Dpod1, an actin/MT crosslinker, must be maintained in the growth cone for correct axon guidance.

Introduction

A growing number of proteins have been implicated in the interactions between actin and MTs (for review, see Rodriguez et al., 2003). At least one actin/MT crosslinker, Kakapo/Short stop, is required for continued axon extension (Lee et al., 2000; Lee and Kolodziej, 2002; Van Vactor et al., 1993); however, whether such proteins have specific roles in axon targeting (turning and branching) is unknown. The machinery responsible for the physical connections or information flow between actin and MTs during axon targeting remains mysterious.

The growth cone is a specialized structure at the tip of a growing axon that integrates extracellular guidance cues into cytoskeletal changes that underlie axon guidance (for review, see Dickson, 2002; Lee and Van Vactor, 2003; Luo, 2002). At the leading edge, finger-like filopodia—consisting of parallel bundles of actin—continuously extend and retract, exploring the immediate environment for guidance cues. Between the filopodia, veil-like membranous sheets, called lamellipodia, contain a complex branched network of actin filaments. Farther back from the lamellipodia, the central region of the growth cone contains MTs that continuously explore the peripheral regions and exhibit dynamic instability, often extending and retracting along actin filaments (Schaefer et al., 2002). When a filopodium encounters an attractive cue, it becomes dilated, and invading MTs are captured and stabilized. These polymerizing MTs then help drive the directional extension of the axon.

Actin and MT structures in growth cones often appear to be crosslinked and depend on each other for structural integrity (Schaefer et al., 2002). Disruption of either actin or MTs in growth cones affects both actin and MTs and can disrupt axon steering (Lin and Forscher, 1993; Rochlin et al., 1999). The molecules underlying this relationship remain unknown.

Pod-1 was isolated from early *C. elegans* extracts based on binding to F-actin, though it is not required for the overall integrity of the actin cytoskeleton. It is a strict maternal effect gene required for all aspects of early embryonic asymmetry and anterior-posterior axis formation (Rappleye et al., 1999), processes that depend on intact MT and actin networks (Lyczak et al., 2002). Pod-1 contains two tandem coronin repeats (Rappleye et al., 1999). Coronin was isolated by MT affinity chromatography and was subsequently shown to bind both actin and MTs (Goode et al., 1999). However, *C. elegans pod-1* has to date not been implicated in MT regulation.

Here, we show that the *Drosophila* homolog of Pod-1, Dpod1, crosslinks actin and MTs in vitro. In S2 cells, Dpod1 colocalizes extensively with newly assembled actin and often colocalizes with MTs that extend out to the lamellar edge or into filopodia. Depolymerization of actin causes Dpod1 to localize to MTs, whereas depolymerization of MTs has no effect on Dpod1 localization. Overexpression of Dpod1 induces dramatic changes in cell shape: long, neurite-like, actin-rich processes form in an actin-dependent (but not MT-dependent) manner and are subsequently invaded by MTs. Interestingly, at their tips, a subset of these processes localize Enabled, an important cytoskeletal regulator that functions together with several different transmembrane receptors (e.g., Robo and UNC-40/DCC) involved in many axon guidance decisions (Bashaw et al., 2000; Gitai et al., 2003; Yu et al., 2002). In developing neurons, Dpod1 is concentrated in growing neurites, where it is especially enriched at the tips of extending axons—often at navigational choice points. The primary defect in embryos completely lacking Dpod1 is aberrant axon targeting. Furthermore, the level of Dpod1 is critical, as postmitotic neuronal overexpression of Dpod1 causes severe defects in axon pathfinding. We propose that Dpod1 is an actin/MT crosslinker that functions in cytoskeletal remodeling during axon navigation and may facilitate the flow of guidance information to cytoskeletal networks.

*Correspondence: ynjan@itsa.ucsf.edu

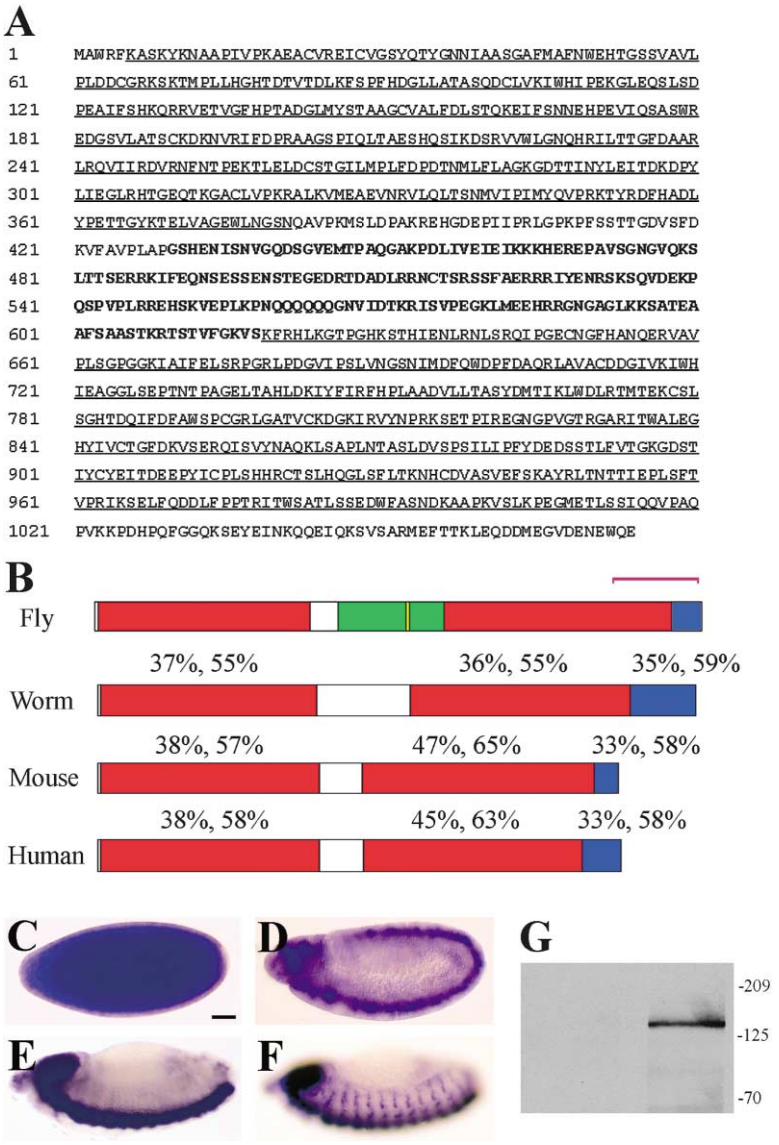

Figure 1. Primary Sequence, Homology Comparison, and Domain Structure of Dpod1

(A) Amino acid sequence of Dpod1. Coronin domains are underlined. Region of MAP1B homology is in bold.

(B) Domain structure of fly, worm, mouse, and human *pod-1* isoforms. Proteins are 1074, 1057, 922, and 925 residues long, respectively. Homology to Dpod1 is indicated (% identity, % similarity) above the coronin domains (red) and the C-terminal tails (blue). The region of homology to the MT binding domain of MAP1B is green, within which the class IK SH3 binding domain is yellow. The region used to generate the anti-Dpod1 antibody is indicated by a bracket.

Panels (C)–(F) show in situ hybridization to wild-type embryos with a *dpod1* probe. Anterior is left, dorsal is up.

(C) Stage 5, (D) Stage 9, (E) Stage 12, deep, (F) Stage 12, superficial. Scale bar equals 30 μm.

(G) Western blot with preimmune serum (left lane, 1:3000 dilution) or anti-Dpod1 (right lane, 1:30,000). 10 μg of a mixed stage (0–16 hr) embryonic extract was loaded in each lane.

Results

Drosophila melanogaster Possesses a Single *pod-1* Gene Expressed in the Nervous System

Sequence analysis of a full-length cDNA for Dpod1 (see Experimental Procedures) showed that the predicted protein has 1074 amino acids (Figure 1A), is 31% identical and 46% similar to *C. elegans* Pod-1, and has a nearly identical domain structure and length (Figure 1B). Thus, like the worm, the fly has a single copy of *pod-1*. Notably, both mice and humans also possess a single *pod-1* gene (Figure 1B, see Supplemental Figure S1A at http://www.neuron.org/cgi/content/full/39/5/779/DC1).

Dpod-1 contains two tandem repeats of coronin homology (Figure 1B), domains that likely mediate F-actin binding (Goode et al., 1999). Each of these domains has three WD repeats, a protein-protein binding motif found in a large number of proteins with diverse functions (Neer et al., 1994). Between the coronin repeats Dpod1 contains a highly charged stretch of 236 amino acids weakly homologous (19% identical, 44% similar) to the MT binding domain of MAP1B (GenBank accession QRMSP1), a MT-associated protein that suppresses MT instability (Noble et al., 1989). The C terminus of Dpod1 has no identifiable domain but is highly conserved (Figure 1B, see Supplemental Figure S1A). Thus, the primary sequence of Dpod1 is consistent with an actin/MT crosslinker.

Using several cDNA antisense probes derived from different regions of the *dpod1* cDNA, we conducted in situ hybridization on 0–16 hr embryos to determine the mRNA expression pattern of *dpod1* during embryogenesis (Figures 1C–1F). Cellularizing (stage 5) embryos demonstrated a ubiquitous maternal contribution of *dpod1* mRNA (Figure 1C). Embryos in early neurogenesis (stage 9) showed high *dpod1* expression in neuroblasts and in their progeny and low expression in the epidermis (Figure 1D). Later on (stage 12), expression was seen in the developing PNS as well as the CNS (Figure 1F). This pattern of high neuronal and low epidermal expression

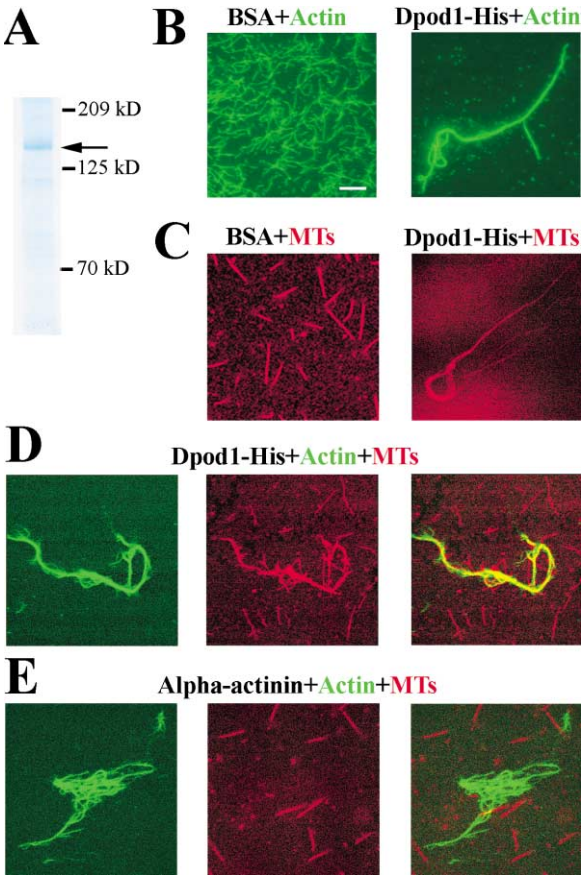

Figure 2. Purified Dpod1 Crosslinks Both Actin and Microtubules

(A) Purified Dpod1-His (arrow) run out by SDS-PAGE and Coomassie stained.

(B) BSA (2.5 μM) fails to bundle Alexa488-phalloidin-stabilized actin (50 nM). Dpod1-His (80–100 nM) causes actin to form bundles. Scale bar equals 5 μm and applies to all panels.

(C) BSA (2.5 μM) fails to crosslink taxol-stabilized rhodaminated MTs (500 nM). Dpod1-His (80–100 nM) crosslinks MTs.

(D) Combination of Dpod1-His (80–100 nM), Alexa488-phalloidin-stabilized actin (50 nM), and taxol-stabilized rhodaminated MTs (500 nM) causes dramatic crosslinking of actin and MTs.

(E) Combination of purified α-actinin (100 nM), Alexa488-phalloidin-stabilized actin (50 nM), and taxol-stabilized rhodaminated MTs (500 nM) aggregates actin but does not crosslink MTs, showing the Dpod1 activity is specific.

persisted throughout embryogenesis. Western blot analysis with an anti-Dpod1 antibody (see Experimental Procedures) on a 0–16 hr embryonic extract showed a single ~130 kDa Dpod1 band, indicating that a single form of Dpod1 was expressed during embryogenesis (Figure 1G).

Purified Dpod1 Crosslinks Actin and Microtubules

To test whether Dpod1 can crosslink actin and MTs, we purified soluble Dpod1 from a stable S2 cell line engineered to inducibly express full-length His-tagged Dpod1 (Figure 2A). When purified Dpod1^{HIS} (80–100 nM) was added to fluorescently labeled phalloidin-stabilized actin filaments (30–60 nM), it rapidly (within minutes) induced the formation of long (20–50 μm), mostly unbranched actin bundles that frequently had bends or curls (Figure 2B, right). Their appearance did not change over time, suggesting that a steady state was reached. When buffer alone or BSA (even at a 25-fold higher concentration) was added to the actin filaments, no bundling activity was observed (Figure 2B, left), demonstrating that the activity was specific. Similarly, when taxol-stabilized fluorescent MTs were combined with purified Dpod1^{HIS} (80–100 nM Dpod1^{HIS}; 500 nM MTs), we saw rapid crosslinking of MTs (Figure 2C, right), whereas no crosslinking occurred with buffer alone or with BSA—even at a 25-fold higher concentration (Figure 2C, left). Thus, Dpod1^{HIS} possessed both actin and MT crosslinking activities.

When Dpod1^{HIS} (80–100 nM) was added simultaneously to phalloidin-stabilized fluorescent actin filaments (30–60 nM) and taxol-stabilized fluorescent MTs (500 nM), a dramatic crosslinking activity was observed in which actin bundles colocalized with MT bundles (Figure 2D). Significantly, when the same experiment was performed with purified α-actinin, a well-characterized actin bundling protein, actin aggregates were seen, but there was no bundling of MTs (Figure 2E). Thus, in vitro, Dpod1 could crosslink actin filaments and MTs, activities that are likely to be significant for the remodeling and coordination of actin and MT networks in dynamic cells.

Dpod1 Colocalizes with a Subset of Actin and MTs in Spreading S2 Cells

To test whether Dpod1 can remodel the cytoskeleton in cells, we began to study Dpod1 in S2 cells, a system that has recently been used to study cytoskeletal dynamics (Rogers et al., 2002). In S2 cells plated and spreading on concanavalinA-coated (conA) cover slips, endogenous Dpod1 localized to sites of new actin polymerization, particularly at the lamellar edge. Costaining fixed cells with Dpod1 and Alexa488-phalloidin showed that Dpod1 was enriched at the edge of ruffling lamellae in an uneven, punctate pattern (Figures 3A–3C). Notably, Dpod1 colocalized with a subset of actin, particularly the newly polymerized actin assembled at the lamellar edge that supports retrograde flow (Figure 3D). Prominent staining was also seen on intralamellar actin filaments and filopodia-like structures (data not shown).

Costaining spreading cells for Dpod1 and Tubulin showed Dpod1 colocalizing with a subset of MTs—especially those whose polymerizing ends were meeting the lamellar edge (Figures 3E–3H). In the rare cells that projected filopodia, Dpod1 accumulated to high levels in those projections (comprised of actin bundles) and colocalized with invading MTs (data not shown). This subcellular localization was consistent with a molecule playing a role in actin/MT interactions.

Disruption of Actin Causes Relocalization of Dpod1 to MTs

To investigate the dependence of Dpod1's subcellular localization on actin and MTs, we treated cells with latrunculin, a drug that leads to the depolymerization of actin microfilaments, or nocodazole, a drug that causes depolymerization of MTs. Nocodazole did not change the subcellular localization of Dpod1 even when MTs were completely depolymerized (Figure 3L); thus, Dpod1 localization was independent of MTs. In contrast, latrun-

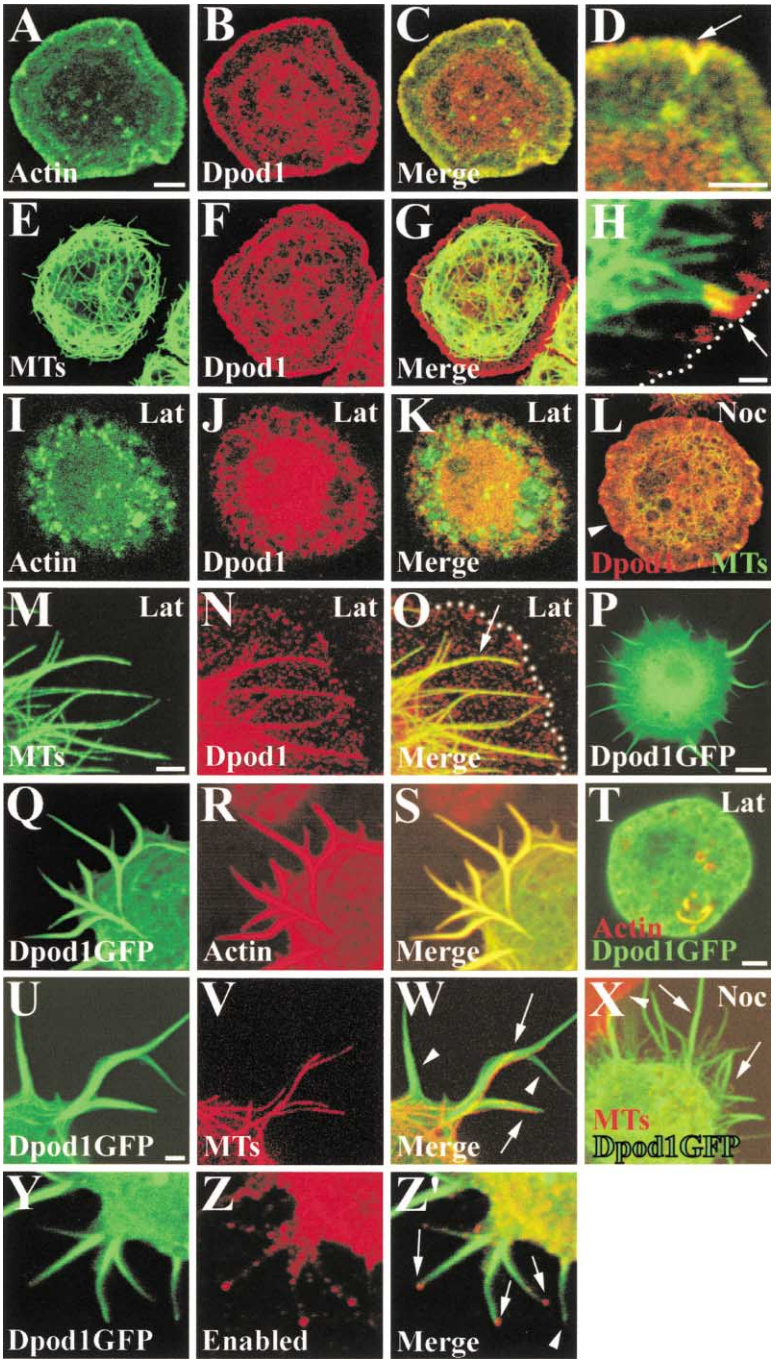

Figure 3. Dpod1 Can Remodel the Cytoskeleton in S2 Cells

Panels (A)–(O) depict untransfected S2 cells, while panels (P)–(Z′) depict cells overexpressing Dpod1GFP. All cells are spreading on conA.

(A–C) A cell stained with Alexa488-Phalloidin (green) and Dpod1 (red) shows extensive colocalization (yellow) of Dpod1 and Actin. Scale bar equals 5 μm and applies to (A)–(C), (E)–(G), and (I)–(L).

(D) Close-up of a lamella shows Dpod1 (red) colocalizes extensively with actin (green) at the cell's edge (arrow). Scale bar equals 3 μm.

(E–H) A cell stained for MTs (green) and Dpod1 (red) shows some colocalization.

(H) A close-up of some MTs approaching the lamellar edge where they colocalize with an accumulation of Dpod1 (arrow). Scale bar equals 0.4 μm

(I–K) Disruption of actin (green) with latrunculin causes Dpod1 (red) to become delocalized from the lamellar edge and dissociated from actin.

(L) Disruption of MTs (green) with nocodazole does not affect Dpod1 (red) localization to the lamellar edge (arrowhead). Compare this to panel (G).

(M–O) Disruption of actin with latrunculin causes Dpod1 (red) to relocalize (arrow) to MTs (green). Scale bar equals 5 μm and applies to (M)–(O), (Q)–(S), and (U)–(Z′).

(P) Live image of a Dpod1GFP-overexpressing cell extending neurite-like processes, an overexpression phenotype since S2 cells are normally round. Scale bar equals 10 μm.

(Q–S) A cell overexpressing Dpod1GFP (green) fixed and stained with rhodamine-phalloidin (red) shows that the processes are actin rich.

(T) A cell expressing Dpod1GFP (green) plated on conA, treated with latrunculin, and then stained for actin (red) shows that the processes are actin dependent. Scale bar equals 2.5 μm.

(U–W) A cell overexpressing Dpod1GFP (green) stained for MTs (red) shows MTs invading some (arrows) but not other (arrowheads) processes.

(X) A cell overexpressing Dpod1GFP (green) treated with nocodazole and stained for MTs (red) shows that the processes (arrows) form in the absence of MTs. A neighboring cell still has some residual MT staining (arrowhead).

(Y–Z′) A cell overexpressing Dpod1GFP (green) fixed and stained for Enabled (red), which localizes to the tips of some of the projections (arrows) but not others (arrowhead).

culin disrupted the actin cytoskeleton and caused Dpod1 to lose its characteristic localization at the lamellar edge (Figures 3I–3K). Costaining for Dpod1 and Tubulin showed that in latrunculin-treated cells, Dpod1 relocalized from actin filaments to MTs (Figures 3M–3O), suggesting that Dpod1 had a high affinity for actin and a lower affinity for MTs or that its association with MTs may have been regulated. This finding, together with the endogenous Dpod1 localization and the observed biochemical activities, was consistent with a role for Dpod1 in the interaction of actin and MTs in dynamic cellular structures.

Dpod1 Can Induce Cytoskeletal Remodeling in a Dose-Dependent Manner

We used RNAi to ask whether depletion of Dpod1 from S2 cells can alter cytoskeletal regulation or dynamics. Although RNAi treatment reduced Dpod1 to undetectable levels (by both immunostaining and Western blot), we observed no changes in cell shape, actin appear-

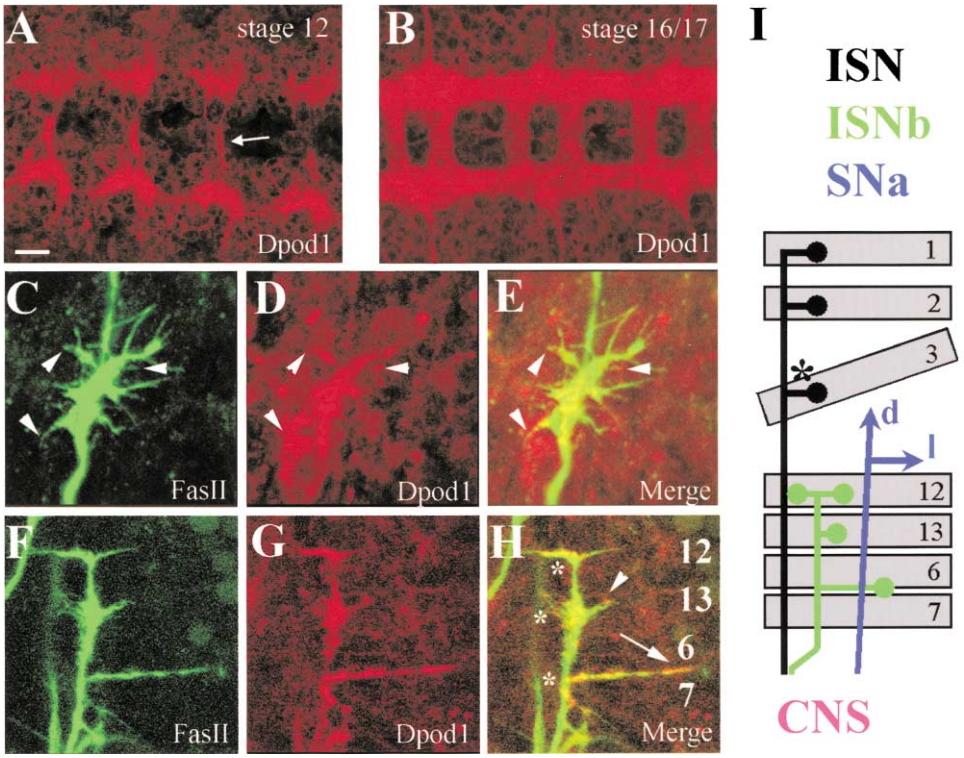

Figure 4. Expression Pattern of Dpod1

(A) Ventral view of the developing CNS of a stage 12 embryo shows Dpod1 on nascent axons crossing the midline (arrow). Scale bar equals 10 μm and applies to all panels.

(B) Same view of a stage 16/17 embryo. Dpod1 remains in mature axons.

Panels (C)–(H) show motorneuron axons in stage 16/17 embryos stained with 1D4/FasII (green) and Dpod1 (red).

(C–E) A close-up view of the first choice point of the intersegmental nerve (ISN). 1D4/FasII outlines the growing axons and shows an extensive network of nascent projections. Dpod1 concentrates at the choice point but not in the axon shafts. Yellow in (E) indicates coincident Dpod1 and 1D4 staining. The arrowheads highlight processes that contain Dpod1.

(F–H) A close-up view of ISNb. Dpod1 concentrates at choice points (asterisks), at the tips of growing axons (arrowhead), and along the length of some axons (arrow).

(I) Schematic of ISN, SNa, and ISNb in a typical abdominal hemisegment. Several muscles are indicated by gray boxes. Dorsal (d) and lateral (l) branches of SNa indicated by small letters. Asterisk indicates region of panels (C)–(E).

ance, or localization, or MT appearance or localization in fixed cells (data not shown). Similarly, when Dpod1-RNAi cells were transfected with ActinGFP or TubulinGFP to assay cytoskeletal dynamics by live imaging, no differences from normal S2 cells were seen. Parameters measured included rate and extent of retrograde actin flow, rate of MT growth and shrinkage, rate of MT catastrophe (transitions from growth or pause to shrinkage per second), rate of MT rescue (transitions from pause or shrinkage to growth per second), and proportions of paused, growing, and shrinking MTs. Thus, Dpod1 does not appear to be necessary for cytoskeletal regulation in S2 cells.

Next, we asked whether Dpod1 overexpression was sufficient to affect cytoskeletal networks. Overexpression of Dpod1GFP caused a dramatic dose-dependent remodeling of cell shape (Figure 3P). Cells expressing high levels of Dpod1GFP (as determined by fluorescence intensity) extended long, neurite-like projections that were sometimes branched (Figure 3P) and were highly dynamic, displaying behaviors such as growth and extension, lateral movement along the cell surface, retrograde flow, and catastrophic collapse and retraction (see Supplemental Movies S1–S3 at http://www.neuron.org/cgi/content/full/39/5/779/DC1). These projections were even observed in cells growing in their culture dish before plating onto conA (data not shown), indicating that their formation did not require the spreading signal provided by conA. In contrast, cells that were untransfected, transfected with ActinGFP, or expressing lower levels of Dpod1GFP were invariably discoid and did not display this dramatic behavior (data not shown).

Staining with rhodamine-phalloidin indicated that the processes not only contained high levels of Dpod1GFP (Figures 3P and 3Q) but were also rich in actin bundles (Figures 3Q–3S). To investigate whether these processes were actin dependent, we treated live, plated cells with latrunculin and observed that the processes did not form (Figure 3T). Similarly, treatment with latrunculin before plating on conA also blocked process formation (data not shown). Taken together with the observation that Dpod1 localization to the lamellar edge in untransfected cells depends on actin (Figures 3I–3K), this shows that the processes are actin dependent.

When fixed and stained for tubulin, many of the processes induced by Dpod1GFP were found to contain

Table 1. Quantification of Axon Defects in ISN, SNa, and ISNb

Genotype (n = hemisegments)	ISN (% abnormal)[a]	SNa (% abnormal)[b]	ISNb (% abnormal)[c]
Loss of Function			
+/+ (wild-type) (n = 193)	0.0	0.0	5.1
Δ*96/Y* (zygotic null)[d] (n = 84)	1.4	8.1	6.9
Δ*96/Y* GLC (maternal and zygotic null) (n = 183)	25.3	55.0	60.1
Δ*96/Y* GLC; *elavGal4$^{4.1}$ UASpod1GFPmyc$^{1\text{-}1\#6}$*/+ (rescue of maternal and zygotic null) (n = 114)	2.9	13.8	32.0
Overexpression[e]			
w; elavGal4$^{4.1}$/elavGal4$^{4.1}$ (n = 104)	1.1	3.3	14.3
w; elavGal4$^{4.1}$ UASpod1GFPmyc$^{1\text{-}1\#6}$/elavGal4$^{4.1}$ UASpod1GFPmyc$^{1\text{-}1\#6}$ (n = 101)	23.3	44.1	56.3

Description of phenotypes is as follows.
[a] Stalling; bypass or failure at any of three dorsal choice points; abnormal defasciculation; abnormal branching.
[b] Missing dorsal or lateral branch; stalling; extra or premature branching; abnormal defasciculation.
[c] Failure to innervate at least one target due to stalling or stopping short; failure of all ISNb axons to defasciculate from ISN.
[d] "Y" indicates Y chromosome.
[e] Experiments conducted at 29°C.

invading MTs (Figures 3U–3W), much like stabilized filopodia in neuronal growth cones (Schaefer et al., 2002). However, the processes were not dependent on MTs, since nocodazole treatment did not block their formation (Figure 3X). Consistent with this result, nearly all the processes extended beyond the ends of invading MTs (Figure 3W); thus, MT polymerization did not drive the extension of these processes.

Also resembling the filopodia of axonal growth cones (Lanier et al., 1999), the tips of a subset of the processes (presumably those that were growing) had a focus of Enabled (Figures 3Y–3Z′), a cytoskeletal regulator that facilitates continued actin polymerization at the barbed ends of actin filaments (Bear et al., 2002), induces cellular projections when overexpressed (Gertler et al., 1996), and functions together with several different receptors (including Robo and UNC-40/DCC) implicated in axon guidance (Bashaw et al., 2000; Gitai et al., 2003; Yu et al., 2002).

Dpod1 Concentrates in the Tips of Growing Axons

To determine the localization of Dpod1 in vivo, we stained embryos for Dpod1. At stage 12, during neurite growth in the CNS, Dpod1 staining was found at high levels in nascent axons (Figure 4A). By stage 16/17, Dpod1 staining was abundant on all axons in the ventral nerve cord (VNC) (Figure 4B). Double labeling with anti-Dpod1 and 1D4/FasII showed Dpod1 staining in axon growth cones and along motor axons (Figures 4C–4H). Interestingly, Dpod1 was especially abundant at important navigational choice points, locations of axon turning or branching where growth cones slow down, enlarge, search the environment for guidance cues, and display precise coordination of actin and MTs (Broadie et al., 1993; Dent and Kalil, 2001; Sink and Whitington, 1991; Van Vactor et al., 1993; Zhou et al., 2002). Although Dpod1 was expressed in all motorneurons, this was particularly noticeable in the ISN and in ISNb. ISN extends from the ventral nerve cord (VNC) to the dorsal musculature where it ramifies axons at three distinct choice points (Figure 4I); at stage 16/17, Dpod1 concentrated at those points (Figures 4C–4E and 5F–5H) in each ISN in all embryos we observed (n > 100). Careful observation showed that Dpod1 appeared to be in a subset of ISN growth cone processes at this stage (Figures 4C–4E, arrowheads). ISNb extends from the VNC into the ventral musculature where axons defasciculate and turn at three distinct choice points to innervate muscles 7, 6, 13, and 12 (Figure 4I). Dpod1 concentrated at the tips and choice points of ISNb axons as well (Figures 4F–4H) in all embryos we observed (n > 100).

dpod1 Is Required for the Fidelity of Axon Targeting

To determine whether Dpod1 has a specific role in axon guidance, we next sought to characterize the mutant phenotype of embryos lacking *dpod1*. *dpod1* is located at 6D1-2 on the X chromosome, a region containing no available deficiencies. Therefore, we generated several null alleles of *dpod1* by imprecise excision of two nearby P elements (see Experimental Procedures). We identified four lethal deletions that remove the entire coding sequence of *dpod1*: Δ17, Δ96, Δ225, and Δ291. This was confirmed by staining for Dpod1 in mutant embryos and mutant mitotic clones (see below). Δ96 was chosen for further study since the only other gene besides *dpod1* it apparently removed was *CG4536*, a putative TRP channel homologous to *C. elegans osm-9* that is not expressed during axonogenesis (data not shown).

In zygotic mutants, although staining with BP102 (an antibody that reveals a regular ladder-like pattern of longitudinal and commissural VNC axons in wild-type embryos) yielded a relatively normal pattern, a low but significant frequency of axon defects was revealed in the motorneurons by 1D4/FasII staining (Table 1). dsRNAi confirmed that the phenotype was in fact due to *dpod1* (data not shown). These defects were most likely due to a primary defect in axon targeting, since we found no defects in neuroblast polarity (determined by examining the asymmetric localization of Bazooka, aPKC, Inscuteable, Miranda, Pon, Prospero, and Numb), mitotic spindle orientation (determined by β-tubulin staining), cell fate determination (determined by Even-skipped staining), or epidermal integrity (determined by Bazooka, DmPar6, aPKC, Armadillo, and Crumbs staining as well as by cuticle analysis of first instar larvae). Nonneuronal features of these embryos were also nor-

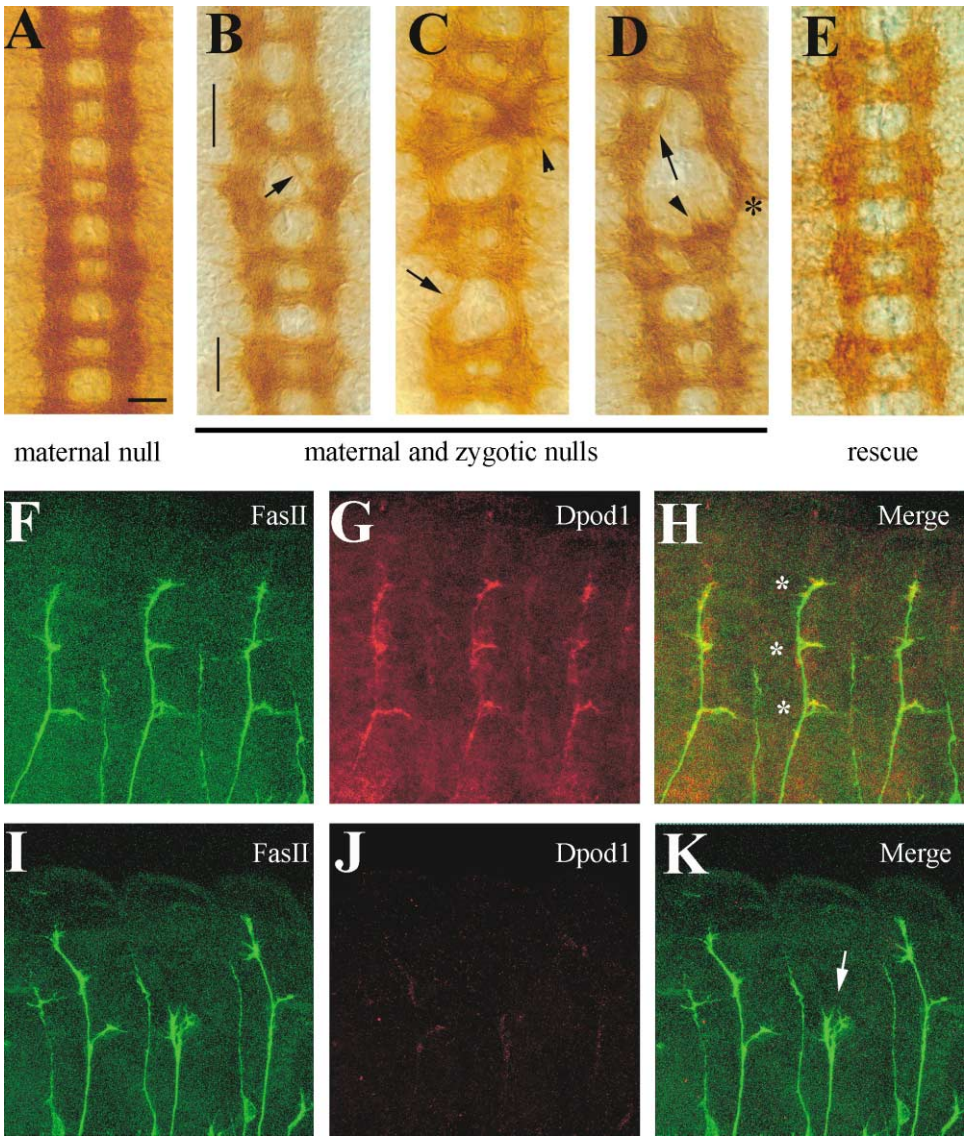

Figure 5. Axon Defects in the Ventral Nerve Cord (VNC) and ISN in Embryos Lacking All Dpod1

Panels (A)–(E) show BP102 staining in filleted stage 16/17 embryos.

(A) A normal VNC axon pattern is seen in embryos lacking maternal (but not zygotic) Dpod1. The same pattern is seen in zygotic *dpod1* mutants, heterozygotes, and wild-type embryos (data not shown). Scale bar equals 10 μm and applies to all panels.

(B–D) Axon defects in embryos lacking both maternal and zygotic *dpod1*.

(B) Midline crossing defect (arrow). Variable spacing between anterior and posterior commissurals (compare vertical lines).

(C) Abnormal longitudinal tract (arrow) and axon tangle (arrowhead).

(D) Misrouting across the midline (arrow), axon tangle (arrowhead), and axons leaving the VNC (asterisk).

(E) An embryo lacking maternal and zygotic *dpod1* and expressing UAS-Dpod1GFP under the control of elavGal4.

(F–H) The dorsal region of three hemisegments of an embryo lacking maternal (but not zygotic) Dpod1 is shown. 1D4/FasII is green and Dpod1 is red. Dorsal ISN choice points indicated by asterisks in (H). Refer to Figure 4I for a schematic.

(I–K) A similar region of an embryo lacking all Dpod1. The middle ISN has stalled and split but still has filopodia (arrow).

mal, including segmentation and muscle pattern (data not shown).

The late pupal lethality of these mutants and the large maternal contribution of *dpod1* mRNA (Figure 1C) indicated that zygotic *dpod1* mutants may still have had significant levels of Dpod1 protein, potentially masking a more severe phenotype. Indeed, stage 16/17 zygotic mutants still contained detectable Dpod1 (see Supplemental Figure S2D at http://www.neuron.org/cgi/content/full/39/5/779/DC1). To examine embryos devoid of all Dpod1 protein, we used the Flp/DFS system to generate germline clone (GLC) embryos that lacked all maternal Dpod1 (see Experimental Procedures). Although GLC embryos that had zygotic Dpod1 often displayed no abnormalities (Figures 5A and 5F–5H) and were viable, GLC embryos lacking zygotic expression had severe CNS axon guidance phenotypes (Table 1, Figures 5 and 6, and see below). These axon guidance phenotypes

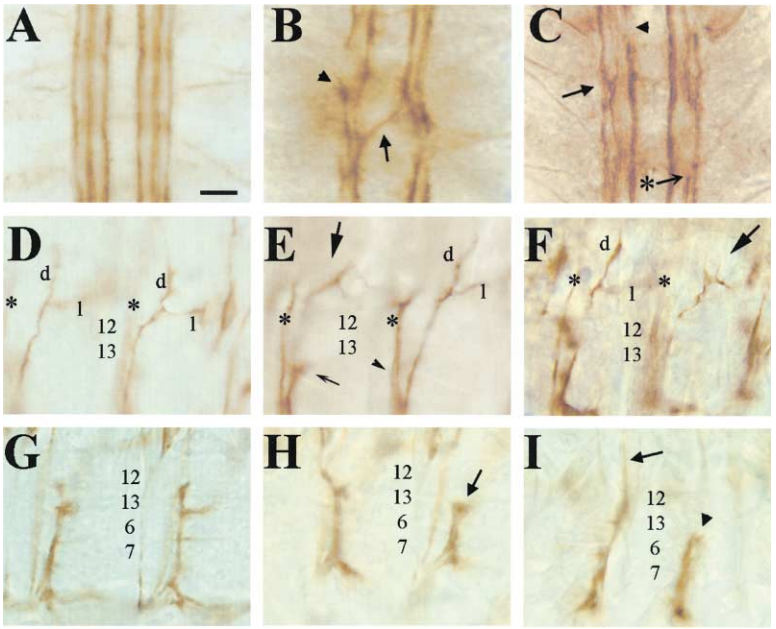

Figure 6. Defects in the VNC, SNa, and ISNb in Embryos Lacking All Dpod1

All panels show 1D4/FasII. (A), (D), and (G) show wild-type embryos. (B), (C), (E), (F), (H), and (I) show embryos lacking all Dpod1.

(A) Normal VNC. Scale bar equals 10 μm and applies to all panels.

(B) Axon breaks (arrowhead) and abnormal midline crossing (arrow).

(C) Collapse of middle and lateral longitudinal tracts (regular arrow) and medial and middle tracts (arrowhead). Axon breaks (arrow with asterisk) are also apparent.

(D–I) Refer to Figure 4I for a schematic.

(D) Two normal SNa patterns. Each has a dorsal (d) and a lateral (l) branch. Asterisks indicate ISN (out of focal plane), and numbers indicate muscles.

(E and F) SNa defects: a missing dorsal branch with abnormal lateral branching (large arrow, E) and stalling/splaying at choice point (arrow, F). Small arrow in (E) shows ISNb stalling at muscle 13 (out of focal plane), and arrowhead shows ISN and ISNb.

(G) Normal ISNb patterns. Muscles are indicated by numbers.

(H) Both nerves (ISNb) fail to extend lateral projections. Arrow indicates ISNb arrested at muscle 13.

(I) Left ISNb extends past muscle 12 (arrow) and only extends weak lateral branches. Right ISNb stops at muscle 13 (arrowhead).

were not accompanied by general defects, as in the case of zygotic mutants, suggesting that Dpod1 in the growth cone is important for axon guidance.

Defects in the Fidelity of Axon Targeting in Embryos Lacking All Dpod1

Embryos lacking all Dpod1 displayed a range of abnormalities in their VNC axons as revealed by BP102 or 1D4/FasII: thinning of longitudinals, abnormal midline crossing and wandering trajectories, axon tangles, axon breaks, collapse or thinning of the anterior and posterior commissurals, and defasciculation (Figures 5B–5D, 6B, and 6C). All embryos devoid of Dpod1 stained with 1D4/FasII ($n > 100$) displayed defects, indicating that the phenotype was fully penetrant. These defects were significantly rescued when these embryos were induced to express Dpod1GFP by *elavGal4*, a postmitotic neural-specific driver (Figure 5E, Table 1), demonstrating that the phenotype was due to the absence of Dpod1 in differentiating neurons and that Dpod1GFP functioned like Dpod1.

To more precisely determine the axonal phenotype by studying isolated nerves, we assayed motorneuron projections by 1D4 staining of embryos lacking all Dpod1. This analysis revealed frequent guidance defects in all the motorneuron projections that normally target body wall muscles: ISN (Figures 5I–5K), SNa (Figures 6E and 6F), ISNb (Figures 6H and 6I), SNc, and ISNd (data not shown). Invariably, ISN axons extended out from the VNC to the region of the first choice point, a distance of many cell diameters. However, in that region, ISN often displayed defects such as stalling/splaying, defasciculation, and failure to innervate targets (Figures 5I–5K, Table 1). This suggested that Dpod1 was required for the guidance of ISN growth cones approaching their targets but was not an essential factor in early axon outgrowth and extension. Normally, SNa defasciculates from the segmental nerve (SN) and projects dorsally in a tight fascicle until reaching the dorsal edge of muscle 12, a choice point where it defasciculates to form a dorsal and a lateral branch (Figures 4I and 6D). In embryos lacking all Dpod1, SNa frequently exhibited defects: a missing or truncated dorsal or lateral branch, arrest/splaying at the choice point, extra branching, or abnormal defasciculation (Table 1, Figures 6E and 6F). Similarly, ISNb axons often displayed various abnormalities, such as failure to innervate the clefts between muscles 6/7 and 12/13, premature arrest (usually around muscle 13), failure to defasciculate from ISN, and bypass of targets (Figures 6H and 6I, Table 1). These ISN, SNa, and ISNb phenotypes were significantly rescued by postmitotic neural expression of Dpod1GFP (Table 1).

In summary, axons devoid of Dpod1 frequently demonstrated aberrant guidance with subsequent failure of target innervation (Table 1), showing that Dpod1 was required for the fidelity of axon turning, branching, or extension past choice points. Importantly, we observed no general problem with early axon outgrowth or extension out to navigational choice points. Moreover, growth cone structure was not obviously disrupted, as filopodia were still seen (Figure 5I). Thus, Dpod1 was not required for filopodia formation in axonal growth cones, an important point since growth cone filopodia are required for steering but not extension of axons (Bentley and Toroian-Raymond, 1986; Marsh and Letourneau, 1984). In addition, expressivity was variable: some nerves reached their targets even without any Dpod1 (Figures 5I–5K and 6, Table 1). Thus, while dispensible for the early steps of axon elongation, Dpod1 was required for the fidelity of axon targeting.

Excess Dpod1 Disrupts Axon Pathfinding

Since Dpod1 was necessary for the fidelity of axon targeting and could remodel the cytoskeleton in S2 cells,

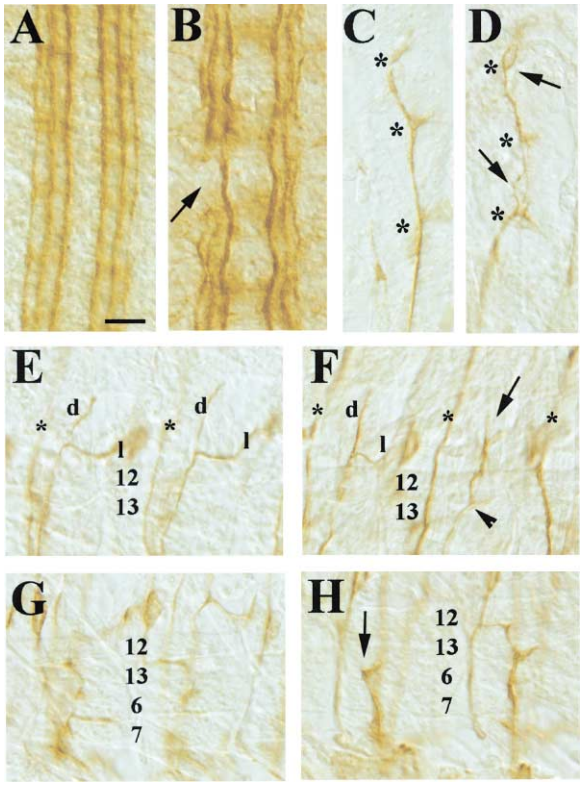

Figure 7. CNS Defects Caused by Postmitotic Neuronal Overexpression of Dpod1

Panels (A), (C), (E), and (G) show *elavG4* embryos; panels (B), (D), (F), and (H) show *elavG4 UAS-dpod1GFPmyc*. All panels show 1D4/FasII.

(A and B) (A) shows a normal pattern, while (B) shows axon irregularities in the VNC (arrow). Scale bar equals 10 μm and applies to all panels.

(C–H) Refer to Figure 4I for schematic.

(C and D) Compare the normal ISN in (C) to that shown in (D). Arrows show defasciculation and splitting. Asterisks represent choice points.

(E) Normal SNa patterns; each SNa has a dorsal (d) and lateral (l) branch that form just dorsal to muscle 12 (indicated by a number). Asterisks indicate ISN, out of the focal plane.

(F) SNa with an abnormal branch (arrowhead) and failure to form dorsal and lateral branches (arrow).

(G and H) Compare the normal ISNb patterns (G) to the stalled ISNb (H). Muscles are indicated by numbers.

we tested whether an overabundance of Dpod1 can disrupt axon targeting. Using two copies each of *elavGal4* and *UAS-Dpod1GFP*, we overexpressed Dpod1GFP postmitotically in neurons and observed multiple, severe axon guidance defects in all axons examined (Table 1, Figure 7). Longitudinal tracts in the VNC exhibited uneven fascicle shapes, abnormal trajectories, axon breaks, and fascicle collapse (Figure 7B). ISN exhibited defasciculation, overbranching, and choice point abnormalities (Figure 7D, Table 1). SNa often showed missing or misplaced branches, abnormal defasciculation, and defective trajectories (Figure 7F). ISNb frequently arrested and failed to innervate targets in the ventral musculature (Figure 7H), remained fasciculated with ISN, or took abnormal trajectories (Table 1). These defects were all consistent with cytoskeletal abnormalities in growth cones leading to defective steering, branching, or extension.

Interestingly, staining of these embryos with 1D4 (even using rapid fixation to preserve filopodia) did not reveal an obvious difference in the number or shape of filopodia (data not shown), suggesting that Dpod1 overexpression had a more subtle effect on cytoskeletal networks in the growth cones than in the S2 cells.

Discussion

Pharmacological and cell biological studies indicate that coordination between actin and MTs is an essential feature of growth cone cytoskeletal dynamics; however, the molecular mechanism for crosslinking actin and MTs and regulating axon targeting in response to guidance cues remains unknown. Using a combination of biochemical, cell biological, and genetic approaches, we have shown *dpod1* to be an essential component of this machinery. We first identified Dpod1 as a candidate actin/MT crosslinker by analyzing its primary sequence. We confirmed this predicted activity by purifying Dpod1 and demonstrating that it could crosslink actin and MTs in vitro. Within spreading S2 cells, Dpod1 localized to a subset of cortical/lamellar actin and MTs and depended on an intact actin cytoskeleton for its localization. Moreover, Dpod1 was able to dramatically remodel the cytoskeleton and influence cell shape; overexpression of Dpod1GFP induced long, dynamic, actin-rich, neurite-like processes that often had a focus of Enabled at their tip and were invaded by MTs.

In vivo Dpod1 was highly enriched in the developing nervous system where it localized to the tips of growing neurites and concentrated in axons at navigational choice points. In embryos completely lacking Dpod1, the fidelity of axon targeting was disrupted, and axons exhibited frequent guidance defects—perhaps due to dysregulation of the growth cone cytoskeleton during turning and/or branching. Interestingly, we did not observe a general defect in early axon outgrowth, since axons invariably extended a long distance from the cell body. Thus, Dpod1 plays a specialized role in the growth cone. Furthermore, axon targeting required proper levels of Dpod1, since postmitotic neuronal overexpression of Dpod1 was sufficient to disrupt axon guidance. Together, these results suggest that Dpod1 is an actin/MT crosslinker that coordinates cytoskeletal dynamics to ensure the fidelity of axon targeting.

Different Roles for Different Actin-MT Crosslinkers in Growth Cones

kakapo/shortstop is an actin-MT crosslinker of the plakin family (for review, see Fuchs and Karakesisoglou, 2001) and is required for continued axon extension in *Drosophila*: embryos homozygous for severe *kak/shot* alleles cannot project sensory axons more than a short distance from the soma and cannot direct motor axons to their targets (Lee et al., 2000; Lee and Kolodziej, 2002). In strong alleles the phenotype is severe, and nearly all axons stop short. Plakins in other systems have been implicated in cell adhesion at sites of mechanical stress; perhaps axons lacking *kak/shot* have adhesive defects or problems with the "clutch" mechanism that enables

axons to grasp a substrate and extend (Jay, 2000; Suter and Forscher, 2000). Although *kak/shot* may be required for axon targeting, its requirement for continued axon extension precludes this knowledge.

In contrast, embryos lacking all Dpod1 can still extend but not target axons, perhaps because of turning and/or branching difficulties. Thus, Dpod1 and Kak/Shot have distinct functions. Additional data support the idea that Kak/Shot—but not Dpod1—plays a primary role in neurite extension: while Dpod1 and Kak/Shot are both found at the tips of dendrites of lateral chordotonal neurons (see Supplemental Figure S1B at http://www.neuron.org/cgi/content/full/39/5/779/DC1), *kak/shot* mutants have difficulty extending these dendrites (Lee et al., 2000), whereas embryos devoid of Dpod1 do not (data not shown).

Furthermore, preliminary genetic interaction data suggest that Dpod1 may function in part to transmit guidance signals to the cytoskeleton. For example, several observations were suggestive of a relationship between Dpod1 and Enabled. (1) Axon defects in embryos devoid of Dpod1 resembled defects in embryos mutant for *enabled (ena)* (Gertler et al., 1995; Wills et al., 1999). (2) Dpod1 overexpression recruited Ena to the ends of the neurite-like projections in S2 cells (Figures 3Y–3Z′). (3) We observed extensive colocalization between Dpod1 and Ena in S2 cells as well as in embryos (data not shown). We therefore tested for genetic interactions between *dpod1*, *ena,* and the *robo* receptor (one of several axon guidance receptors that directly binds to Ena) to ask whether the genes might function together in midline repulsion, a specific axon guidance decision that involves Robo and Ena (Bashaw et al., 2000). Indeed, we found that while *dpod1* zygotic mutants, *ena* heterozygotes, or *robo* heterozygotes did not exhibit midline crossing errors, when gene dosages of *ena* or *robo* were reduced simultaneously with *dpod1*, frequent (i.e., in approximately 30% of abdominal segments) midline crossing errors were observed (unpublished data, M.E.R. and Y.-N.J.).

If Dpod1 functions together with guidance signaling molecules such as Robo and Ena, one possible difference between Dpod1 and Kak/Shot is that Dpod1 may have a more subtle or regulated function in the transmission of guidance information from receptors to the cytoskeleton, rather than a constitutive structural role.

Relating Dpod1's Functions in Cultured Cells to Axonal Growth Cones

In S2 cells, high levels of Dpod1GFP dramatically remodeled both the actin and MT cytoskeletal networks to cause the outgrowth of dynamic, actin-rich, actin-dependent processes. Many of these processes localized Ena to their tips and were invaded by MTs, much like the dilated filopodia of axonal growth cones that have encountered chemoattractant cues. Consistent with this, postmitotic neuronal overexpression of Dpod1 in embryos caused defects in axon targeting. However, the axons in these embryos did not appear significantly different from wild-type: even when rapid fixation techniques were employed to preserve filopodia, we did not observe the same kind of dramatic changes in cell shape observed in cell culture overexpressors. However, *Drosophila* growth cones are extremely small; it remains possible that very careful live imaging may reveal a dynamic difference. Also, while expression levels in the overexpression embryos were high enough to alter axon targeting (presumably by affecting signaling and/or the cytoskeleton in a subtle or regulated way at choice points), the levels achieved may not have been high enough to strongly affect cell shape. In fact, in the overexpression embryos, we still observed specific Dpod1 localization to choice points—suggesting that the machinery that localizes Dpod1 was not saturated in spite of overexpression (data not shown). Thus, while high levels of overexpression can be achieved in S2 cells to drastically alter cell shape, lower levels of overexpression are sufficient to affect navigating growth cones in embryos.

We were surprised that reducing Dpod1 to undetectable levels by RNAi had no apparent effect on cytoskeletal dynamics in S2 cells. Notably, depletion of several other molecules that function as important cytoskeletal regulators in growth cones (such as Ena and Kak/Shot) also has no effect on S2 cell cytoskeletal dynamics (S.L.R. and R.D.V., unpublished data), perhaps because S2 cells are nonpolarized nonmotile phagocytes and are therefore different from neurons (Ramet et al., 2002). Whereas S2 cells can inform us about Dpod1's capabilities to remodel cytoskeletal networks and recruit regulatory components (e.g., Ena) to the tips of cellular processes, it is conceivable that Dpod1 performs these functions in neurons in response to signaling information that S2 cells do not receive.

Dpod1 and the Fidelity of Axon Guidance: Two Models for Dpod1 Function

Although embryos devoid of all Dpod1 had frequent axon targeting defects, some axons were still able to reach their targets. Thus, Dpod1 is not absolutely required for axon targeting but instead ensures its fidelity. Perhaps Dpod1 has a regulatory role, or perhaps it functions redundantly with other molecules in growth cones. At least two models for the function of Dpod1 could account for the observed defects. They are not mutually exclusive. First, Dpod1 may function as part of an "information scaffold" that links important signaling molecules to the actin and MT networks. As part of an information scaffold, Dpod1 may function as a bridge that physically connects signaling molecules downstream of guidance receptors with actin and MTs. In this way, Dpod1 might facilitate the flow of extracellular guidance information to the cytoskeleton. Second, Dpod1 could also play a structural role by stabilizing cytoskeletal networks or certain cytoskeletal structures in growth cones.

Interestingly, Dpod1 contains a +xxPxxP domain in its central region (Figure 1B), a class 1K SH3 binding domain (Cesareni et al., 2002), as well as several other PXXP motifs that may bind to SH3 domain-containing proteins. Perhaps Dpod1 interacts with one or more of the several known SH3 domain-containing signaling proteins that play important roles in many axon guidance decisions.

As a cytoskeletal crosslinker, Dpod1 could provide structural support to the growth cone cytoskeleton and thereby enable guidance information to be effectively

translated into concerted cytoskeletal changes. Unfortunately, *Drosophila* growth cones are too small to allow a detailed description of the growth cone cytoskeleton, and we cannot easily determine what subtle effects loss of Dpod1 may have on growth cone cytoskeletal networks. However, our biochemical experiments show that Dpod1 possesses three distinct biochemical activities: actin bundling, MT crosslinking, and actin/MT crosslinking. Any of these may be important in the growth cone.

Studies have shown that actin bundles are key elements in growth cone steering. Stabilization of actin bundles in a subregion of the growth cone anticipates attractive turning; conversely, focal loss of actin bundling induces local growth cone collapse and repulsive turning (Zhou et al., 2002). Moreover, growth cone filopodia, while not required for continued axon extension, apparently determine the direction of axon growth (Bentley and Toroian-Raymond, 1986; Marsh and Letourneau, 1984). As growth cones devoid of all Dpod1 still have filopodia (Figures 4I–4K), Dpod1 may play a role in regulating or modulating actin bundles or filopodia in vivo.

Many studies have also illustrated the importance of MTs and MT regulatory proteins in axon guidance (Buck and Zheng, 2002; Gonzalez-Billault et al., 2001; Hummel et al., 2000; Yu et al., 2001). In fact, local stabilization of MTs can induce axon attraction, while local destabilization of MTs can induce repulsion (Buck and Zheng, 2002). Since Dpod1 localizes to MTs at the lamellar edge and can crosslink MTs in vitro, it may contribute to the capture and stabilization of MT ends or other aspects of MT regulation in growth cones.

Increasing evidence has also emerged demonstrating that actin and MTs are precisely coordinated and highly regulated in growth cones (Dent and Kalil, 2001; Kabir et al., 2001; Lee and Kolodziej, 2002; Schaefer et al., 2002). Polymerizing MTs preferentially extend along actin bundles during attractive growth, and MTs are probably linked to actin bundles as they undergo retrograde flow during filopodial retraction (Schaefer et al., 2002). Pharmacological disruption of actin affects MT organization, and vice versa (Lin and Forscher, 1993; Rochlin et al., 1999). Disruption of actin/MT crosslinking would be expected to disrupt axonal steering but not extension. Thus, Dpod1 may be involved in actin/MT crosslinking in the growth cone. This would be consistent with the axon defects in embryos lacking Dpod1, the observations in S2 cells, and the in vitro experiments. In support of this, as actin/MT interactions are known to be required in migrating cells (Waterman-Storer and Salmon, 1999; Zigmond, 1999), we observed that embryos lacking Dpod1 exhibited PNS abnormalities consistent with cell migration defects. Normally, the lateral chordotonal neurons migrate to become evenly aligned along the dorsal-ventral (D/V) axis; however, in embryos lacking all Dpod1, these neurons varied in their D/V position (data not shown). Incidentally, this phenotype is also seen in *ena* mutants (Gertler et al., 1995).

Concluding Remarks

Our study has identified Dpod1 as an actin/MT crosslinker that can remodel the cytoskeleton and play an essential role in ensuring the fidelity of axon targeting. Dpod1 is highly conserved across evolution (Figure 1B) and may be important in neural development in different organisms. Mice and humans each possess a single *pod-1*. Interestingly, mouse *pod-1* is expressed in the developing nervous system, with high levels in the dorsal root ganglia and neural tube (data not shown). Subsequent work may reveal whether mammals and insects utilize *pod-1* in similar ways during neural development.

Experimental Procedures

Molecular Cloning and Sequence Analysis

Following the release of the *Drosophila* genomic sequence by the Berkeley *Drosophila* Genome Project (BDGP), we used the BLAST sequence analysis program to find a fly ortholog of *pod-1*, CG4532 (*dpod1*). Dpod1 ESTs were identified by searching the BDGP EST collection and then obtained from Research Genetics. We sequenced both strands of a *dpod1* EST, LD15267, and found it to be full-length (stop codon 9 bp upstream of the ATG) with no major differences from the predicted cDNA of CG4532. Homology between Dpod1 homologs was determined using the ClustalW multiprotein alignment tool. Sequence similarity between Dpod1 and MAP1B was determined using the NCBI Blast-2-Sequences tool.

To generate the Dpod1-Cterm plasmid, a StuI/XhoI fragment of LD15267 was cloned into pGEX 4T-3 cut with SmaI/XhoI. pUAST-Dpod1 was made by cloning the NotI/KpnI insert from LD15267 into pUAST. pUAST-Dpod1GFPmyc was made in two steps by (1) excising the Bazooka sequence from a pUAST-BazookaGFPmyc construct (gift of Y. Hong) and replacing it with a NotI/NheI fragment of LD15267 (encoding most of Dpod1), and then (2) PCR amplifying and inserting the remainder of Dpod1 (without the stop codon). pUAST-Dpod1-RNAi was made by cloning a MluI/NotI band from LD15267 into pUAST cut with NotI. Cloning of pMT Dpod1-V5HisA was done in two steps by first cloning an EcoRI fragment with most of the coding sequence of Dpod1 into pMT V5 His A (Invitrogen) and then inserting the remaining 19 amino acids (without the stop codon) of Dpod1 using PCR. All constructs were verified by DNA sequencing.

In Situ Hybridization

In situ hybridization was done on 0–16 hr embryos by generating digoxygenin-labeled ~500 bp unique cDNA probes (Tautz and Pfeifle, 1989).

Antibody Production and Immunohistochemistry

GST-Dpod1-Cterm (a GST fusion protein to the 128 C-terminal amino acids of Dpod1, a region with no homology to other fly proteins) was made in BL21 *E. coli* cells and purified on glutathione-conjugated sepharose beads (Amersham). Guinea pig antibodies were then generated by Strategic Biosolutions. Specificity was confirmed in several ways. First, anti-Dpod1 staining of wing imaginal discs from several lines of transgenic flies expressing UAS-dpod1 under the control of the patched-Gal4 driver revealed a patched-Gal4 expression pattern of Dpod1 superimposed on a lower level of epithelial staining. Also, the antibody (but not preimmune serum) specifically recognized in vitro translated protein synthesized from the *dpod1* cDNA clone LD15267. Moreover, Western blots showed that the single Dpod1 band present in S2 cell extracts disappeared after 1 week of treatment with *dpod1* RNAi.

The anti-Dpod1 antibodies were used in immunohistochemistry at a dilution of 1:1500 and on Western blots at a dilution up to 1:30,000. Other antibodies used include 1D4 (1:10), BP102 (1:10), M18 (1:10), Rb anti-Miranda (1:1000), Rb anti-Insc (1:1000), Rb anti-Bazooka N-term (1:1000), Rb anti-aPKC (1:1000), Rb anti-Dmpar6 (1:500), Rb anti-Pins (1:1000), Rb anti-Numb (1:1000), Rb anti-Pon (1:1000), Rb anti-prospero (1:1000), Rb anti-staufen (1:1000), and mouse anti-tubulin (1:1000) (Sigma).

Biochemistry and Actin/Microtubule Bundling Assays

Dpod1-His was purified according to instructions from Invitrogen's DES kit. Cells from a stable pMT Dpod1-V5 HisA S2 cell line were induced in culture media with 1 mM CuSO4 for 4–8 days, resus-

pended in cold PBS + 1% Triton-X100 + 10 mM imidazole + 1× Complete protease inhibitors (Roche), agitated for 1 hr at 4°C, and spun 10 min at 4000 × g. The supernantant was kept. Prewashed Ni-NTA agarose beads (Qiagen) were added; binding continued at 4°C for 3 hr. A column was made and then washed (20 bed volumes per wash), first in 10 mM TrisHCl (pH 7.5) + 50 mM KCl + 20 mM imidazole + 1% TritonX100, then in 10 mM TrisHCl (pH 7.5) + 300 mM KCl + 20 mM imidazole, and lastly in 10 mM TrisHCl (pH 7.5) + 50 mM KCl + 20 mM imidazole. Dpod1-His was eluted in 10 mM TrisHCl (pH 7.5) + 50 mM KCl + 250 mM imidazole. 1 mM DTT and 0.1% NaN3 were added. The protein was stored on ice or frozen in liquid N_2 with 10% glycerol and kept at −80°C. Imidazole was dialyzed down to 10 mM, but results were unaffected by 250 mM imidazole. Purified lyophilized α-actinin (Cytoskeleton) was reconstituted to 2.5 mg/ml in 20 mM NaCl + 20 mM TrisHCl (pH 7.2) + 5% sucrose + 1% dextran + 1 mM β-mercaptoethanol. Actin was purified from *Acanthamoeba* (MacLean-Fletcher and Pollard, 1980). Actin filaments were polymerized for 30 min at room temperature by adding of 0.1 vol of 10× KMEI buffer to monomeric actin, followed by the addition of 1.2 molar excess of Alexa488-phalloidin. MTs were prepared by polymerizing rhodaminated tubulin and stabilizing them with taxol. Bundling assays were done by combining Alexa488-phalloidin stabilized actin (100 nM final), taxol-stabilized rhodaminated MTs (500 nM final), and protein (BSA, α-actinin, or Dpod1-His); mixing and waiting for 2–10 min at room temperature; spotting on a slide; and viewing.

S2 Cell Culture

All S2 cell culture experiments were done as described (Rogers et al., 2002) and as indicated by Invitrogen's *Drosophila* Expression System (DES) manual. For latrunculin experiments, spreading cells were treated with 100 nM latrunculin dissolved in DMSO or DMSO as a control for 30 min before fixing.

Fly Stocks and Genetics

Flies were grown on standard media at 25°C. *ena*^{GC5} and *ena*^{GC8} flies were obtained from D. Van Vactor. *robo*^{1} and *robo*^{5} flies were obtained from G. Bashaw. P element insertions EP(X)1613 and P{GT1}BG02604 were obtained from the Bloomington Stock Center. EP(X)1613 is a viable fertile line inserted ~14 kB upstream of the *dpod1* coding sequence and within 500 bp of the gene *C(3)G*, a guanine nucleotide exchange factor (GEF) for the small GTPases Rap1 and Ras (Ishimaru et al., 1999; Mochizuki et al., 2000; Ohba et al., 2001). P{GT1}BG02604 is a viable fertile line inserted ~300 bases upstream of *dpod1*. Excisions of EP(X)1613 (Δ225 and Δ291) were generated by screening for loss of eye color and hemizygous lethality. Excisions of P{GT1}BG02604 (Δ17 and Δ96) were generated by screening for loss of eye color and lethality over Δ225. A genomic duplication of 6C8-6D11, *Dp(1;Y)dx*$^{+5}$*y*$^{+}$, was obtained from the Bloomington Stock Center and was used to carry lethal alleles in males. The extent of deletions was determined by PCR analysis on mutant DNA using primers based on the *Drosophila* genome sequence. In addition to *dpod1*, Δ225 and Δ291 disrupted *C(3)G*, indicated by PCR and in situ hybridization. Δ225 and Δ291 caused late larval lethality, and hemizygous larvae were stunted in size but had no other obvious morphological defects. In addition to *dpod1*, Δ17, Δ96, and Δ291 disrupted *CG4536*. Δ17 and Δ96 were pupal lethal, and mutants were normally sized with no obvious morphological defects. These data are summarized in Supplemental Figure S2 at http://www.neuron.org/cgi/content/full/39/5/779/DC1. Δ17, Δ96, Δ225, and Δ291 all failed to complement each other and were rescued by *Dp(1;Y)dx*$^{+5}$*y*$^{+}$.

GLCs were generated by heat shocking third instar *yw ΔDpod1 Frt9-2 / OvoD2 v Frt9-2; pr pwn hs-flp / hsflp* larvae, crossing the adults to *w*$^{-}$ males (or *yw; elavG4 UAS-Dpod1GFPmyc* males for the rescue), and collecting embryos. GLCs lacking all Dpod1 were identified by an absence of immunoreactivity for Dpod1 or M18 (anti-Sxl, expressed only in females).

UAS-Dpod1, UAS-Dpod1GFPmyc, and UAS-Dpod1-RNAi transgenic flies were generated by injecting pUAST-Dpod1, pUAST-Dpod1GFPmyc, and pUAST-Dpod1-RNAi DNA (with Δ2–3 DNA) into *w*$^{-}$ embryos.

Acknowledgments

We thank members of the Jan lab and Vale lab for helpful discussions and advice. We also thank Graeme Davis, Wes Grueber, Mike Kim, Fabrice Roegiers, Jenny Roost, and Songhai Shi for insightful comments on the manuscript. Yang Hong provided the pUAST-BazGFP-myc plasmid. Mike Kim provided invaluable technical advice. Mark Dayel and Dyche Mullins kindly provided fluorescent actin and generous advice for experiments shown in Figure 2. Susan Younger helped significantly with fly genetics. Tong Cheng assisted with cell culture. We thank the Bloomington Stock Center for fly stocks and the Developmental Studies Hybridoma Bank for antibodies. M.E.R. is supported by the UCSF Medical Scientist Training Program, the Alcohol and Substance Abuse Research Program at the Gallo Center, and the UCSF Department of Neurology. L.Y.J., Y.-N.J., and R.D.V. are HHMI investigators. S.L.R. is an HHMI associate.

Received: April 4, 2003
Revised: June 3, 2003
Accepted: July 30, 2003
Published: August 27, 2003

References

Bashaw, G.J., Kidd, T., Murray, D., Pawson, T., and Goodman, C.S. (2000). Repulsive axon guidance: Abelson and Enabled play opposing roles downstream of the roundabout receptor. Cell *101*, 703–715.

Bear, J.E., Svitkina, T.M., Krause, M., Schafer, D.A., Loureiro, J.J., Strasser, G.A., Maly, I.V., Chaga, O.Y., Cooper, J.A., Borisy, G.G., and Gertler, F.B. (2002). Antagonism between Ena/VASP proteins and actin filament capping regulates fibroblast motility. Cell *109*, 509–521.

Bentley, D., and Toroian-Raymond, A. (1986). Disoriented pathfinding by pioneer neurone growth cones deprived of filopodia by cytochalasin treatment. Nature *323*, 712–715.

Broadie, K., Sink, H., Van Vactor, D., Fambrough, D., Whitington, P.M., Bate, M., and Goodman, C.S. (1993). From growth cone to synapse: the life history of the RP3 motor neuron. Dev. Suppl., 227–238.

Buck, K.B., and Zheng, J.Q. (2002). Growth cone turning induced by direct local modification of microtubule dynamics. J. Neurosci. *22*, 9358–9367.

Cesareni, G., Panni, S., Nardelli, G., and Castagnoli, L. (2002). Can we infer peptide recognition specificity mediated by SH3 domains? FEBS Lett. *513*, 38–44.

Dent, E.W., and Kalil, K. (2001). Axon branching requires interactions between dynamic microtubules and actin filaments. J. Neurosci. *21*, 9757–9769.

Dickson, B.J. (2002). Molecular mechanisms of axon guidance. Science *298*, 1959–1964.

Fuchs, E., and Karakesisoglou, I. (2001). Bridging cytoskeletal intersections. Genes Dev. *15*, 1–14.

Gertler, F.B., Comer, A.R., Juang, J.L., Ahern, S.M., Clark, M.J., Liebl, E.C., and Hoffmann, F.M. (1995). enabled, a dosage-sensitive suppressor of mutations in the *Drosophila* Abl tyrosine kinase, encodes an Abl substrate with SH3 domain-binding properties. Genes Dev. *9*, 521–533.

Gertler, F.B., Niebuhr, K., Reinhard, M., Wehland, J., and Soriano, P. (1996). Mena, a relative of VASP and *Drosophila* Enabled, is implicated in the control of microfilament dynamics. Cell *87*, 227–239.

Gitai, Z., Yu, T.W., Lundquist, E.A., Tessier-Lavigne, M., and Bargmann, C.I. (2003). The netrin receptor UNC-40/DCC stimulates axon attraction and outgrowth through enabled and, in parallel, Rac and UNC-115/AbLIM. Neuron *37*, 53–65.

Gonzalez-Billault, C., Avila, J., and Caceres, A. (2001). Evidence for the role of MAP1B in axon formation. Mol. Biol. Cell *12*, 2087–2098.

Goode, B.L., Wong, J.J., Butty, A.C., Peter, M., McCormack, A.L., Yates, J.R., Drubin, D.G., and Barnes, G. (1999). Coronin promotes the rapid assembly and cross-linking of actin filaments and may

link the actin and microtubule cytoskeletons in yeast. J. Cell Biol. *144*, 83–98.

Hummel, T., Krukkert, K., Roos, J., Davis, G., and Klambt, C. (2000). *Drosophila* Futsch/22C10 is a MAP1B-like protein required for dendritic and axonal development. Neuron *26*, 357–370.

Ishimaru, S., Williams, R., Clark, E., Hanafusa, H., and Gaul, U. (1999). Activation of the *Drosophila* C3G leads to cell fate changes and overproliferation during development, mediated by the RAS-MAPK pathway and RAP1. EMBO J. *18*, 145–155.

Jay, D.G. (2000). The clutch hypothesis revisited: ascribing the roles of actin-associated proteins in filopodial protrusion in the nerve growth cone. J. Neurobiol. *44*, 114–125.

Kabir, N., Schaefer, A.W., Nakhost, A., Sossin, W.S., and Forscher, P. (2001). Protein kinase C activation promotes microtubule advance in neuronal growth cones by increasing average microtubule growth lifetimes. J. Cell Biol. *152*, 1033–1044.

Lanier, L.M., Gates, M.A., Witke, W., Menzies, A.S., Wehman, A.M., Macklis, J.D., Kwiatkowski, D., Soriano, P., and Gertler, F.B. (1999). Mena is required for neurulation and commissure formation. Neuron *22*, 313–325.

Lee, S., and Kolodziej, P.A. (2002). Short Stop provides an essential link between F-actin and microtubules during axon extension. Development *129*, 1195–1204.

Lee, H., and Van Vactor, D. (2003). Neurons take shape. Curr. Biol. *13*, R152–R161.

Lee, S., Harris, K.L., Whitington, P.M., and Kolodziej, P.A. (2000). short stop is allelic to kakapo, and encodes rod-like cytoskeletal-associated proteins required for axon extension. J. Neurosci. *20*, 1096–1108.

Lin, C.H., and Forscher, P. (1993). Cytoskeletal remodeling during growth cone-target interactions. J. Cell Biol. *121*, 1369–1383.

Luo, L. (2002). Actin cytoskeleton regulation in neuronal morphogenesis and structural plasticity. Annu. Rev. Cell Dev. Biol. *18*, 601–635.

Lyczak, R., Gomes, J.E., and Bowerman, B. (2002). Heads or tails: cell polarity and axis formation in the early *Caenorhabditis elegans* embryo. Dev. Cell *3*, 157–166.

MacLean-Fletcher, S., and Pollard, T.D. (1980). Mechanism of action of cytochalasin B on actin. Cell *20*, 329–341.

Marsh, L., and Letourneau, P.C. (1984). Growth of neurites without filopodial or lamellipodial activity in the presence of cytochalasin B. J. Cell Biol. *99*, 2041–2047.

Mochizuki, N., Ohba, Y., Kobayashi, S., Otsuka, N., Graybiel, A.M., Tanaka, S., and Matsuda, M. (2000). Crk activation of JNK via C3G and R-Ras. J. Biol. Chem. *275*, 12667–12671.

Neer, E.J., Schmidt, C.J., Nambudripad, R., and Smith, T.F. (1994). The ancient regulatory-protein family of WD-repeat proteins. Nature *371*, 297–300.

Noble, M., Lewis, S.A., and Cowan, N.J. (1989). The microtubule binding domain of microtubule-associated protein MAP1B contains a repeated sequence motif unrelated to that of MAP2 and tau. J. Cell Biol. *109*, 3367–3376.

Ohba, Y., Ikuta, K., Ogura, A., Matsuda, J., Mochizuki, N., Nagashima, K., Kurokawa, K., Mayer, B.J., Maki, K., Miyazaki, J., and Matsuda, M. (2001). Requirement for C3G-dependent Rap1 activation for cell adhesion and embryogenesis. EMBO J. *20*, 3333–3341.

Ramet, M., Manfruelli, P., Pearson, A., Mathey-Prevot, B., and Ezekowitz, R.A. (2002). Functional genomic analysis of phagocytosis and identification of a *Drosophila* receptor for *E. coli*. Nature *416*, 644–648.

Rappleye, C.A., Paredez, A.R., Smith, C.W., McDonald, K.L., and Aroian, R.V. (1999). The coronin-like protein POD-1 is required for anterior-posterior axis formation and cellular architecture in the nematode *Caenorhabditis elegans*. Genes Dev. *13*, 2838–2851.

Rochlin, M.W., Dailey, M.E., and Bridgman, P.C. (1999). Polymerizing microtubules activate site-directed F-actin assembly in nerve growth cones. Mol. Biol. Cell *10*, 2309–2327.

Rodriguez, O.C., Schaefer, A.W., Mandato, C.A., Forscher, P., Bement, W.M., and Waterman-Storer, C.M. (2003). Conserved microtubule-actin interactions in cell movement and morphogenesis. Nat. Cell Biol. *5*, 599–609.

Rogers, S.L., Rogers, G.C., Sharp, D.J., and Vale, R.D. (2002). *Drosophila* EB1 is important for proper assembly, dynamics, and positioning of the mitotic spindle. J. Cell Biol. *158*, 873–884.

Schaefer, A.W., Kabir, N., and Forscher, P. (2002). Filopodia and actin arcs guide the assembly and transport of two populations of microtubules with unique dynamic parameters in neuronal growth cones. J. Cell Biol. *158*, 139–152.

Sink, H., and Whitington, P.M. (1991). Pathfinding in the central nervous system and periphery by identified embryonic *Drosophila* motor axons. Development *112*, 307–316.

Suter, D.M., and Forscher, P. (2000). Substrate-cytoskeletal coupling as a mechanism for the regulation of growth cone motility and guidance. J. Neurobiol. *44*, 97–113.

Tautz, D., and Pfeifle, C. (1989). A non-radioactive in situ hybridization method for the localization of specific RNAs in *Drosophila* embryos reveals translational control of the segmentation gene hunchback. Chromosoma *98*, 81–85.

Van Vactor, D.V., Sink, H., Fambrough, D., Tsoo, R., and Goodman, C.S. (1993). Genes that control neuromuscular specificity in *Drosophila*. Cell *73*, 1137–1153.

Waterman-Storer, C.M., and Salmon, E. (1999). Positive feedback interactions between microtubule and actin dynamics during cell motility. Curr. Opin. Cell Biol. *11*, 61–67.

Wills, Z., Bateman, J., Korey, C.A., Comer, A., and Van Vactor, D. (1999). The tyrosine kinase Abl and its substrate enabled collaborate with the receptor phosphatase Dlar to control motor axon guidance. Neuron *22*, 301–312.

Yu, W., Ling, C., and Baas, P.W. (2001). Microtubule reconfiguration during axogenesis. J. Neurocytol. *30*, 861–875.

Yu, T.W., Hao, J.C., Lim, W., Tessier-Lavigne, M., and Bargmann, C.I. (2002). Shared receptors in axon guidance: SAX-3/Robo signals via UNC-34/Enabled and a Netrin-independent UNC-40/DCC function. Nat. Neurosci. *5*, 1147–1154.

Zhou, F.Q., Waterman-Storer, C.M., and Cohan, C.S. (2002). Focal loss of actin bundles causes microtubule redistribution and growth cone turning. J. Cell Biol. *157*, 839–849.

Zigmond, S.H. (1999). A method for movement. Nat. Cell Biol. *1*, E12.